

Formation of the $\Sigma(2030)$ resonance in the reactions $K^-n \rightarrow \Sigma^- \pi^0$ and $K^-n \rightarrow \Sigma^0 \pi^-$ in the center-of-mass energy interval 1850–2150 MeV

D. P. Goyal and A. V. Sodhi

Department of Physics and Astrophysics, University of Delhi, Delhi-110007, India

(Received 7 December 1976)

A partial-wave analysis of the pure isospin $I = 1$ reactions $K^-n \rightarrow \Sigma^- \pi^0$ and $K^-n \rightarrow \Sigma^0 \pi^-$ in the center-of-mass energy range 1850–2150 MeV is reported. The decay mode $\Sigma(2030) \rightarrow \Sigma \pi$ is observed with a branching ratio x , given by $e^{i\phi}(x, x_e)^{1/2} = -0.085 \pm 0.02$, where x_e is the elasticity and ϕ is the relative phase of the resonance with the phase of $\Sigma(1765)$ taken to be zero.

I. INTRODUCTION

Of the many Σ resonances¹ known in the energy region 1850–2200 MeV, $\Sigma(2030)$ with spin parity $J^P = \frac{1}{2}^+$ is well established. However, only the $\bar{K}N$ and $\Lambda\pi$ decay modes for this resonance are well determined. The branching fraction for these two modes combined is $\approx 40\%$. The $\Sigma\pi$ decay mode of this resonance is poorly known at present.^{2,3} Keeping this in view, we did the partial-wave analysis of the pure isospin $I = 1$ reactions $K^-n \rightarrow \Sigma^- \pi^0$ and $K^-n \rightarrow \Sigma^0 \pi^-$ in the center-of-mass (c.m.) energy range from 1850 to 2150 MeV.

In this paper we present the results of this analysis. The data consist of the cross sections and angular distributions as a function of energy. The polarization of the Σ could not be obtained because of the lack of information on the decay properties of Σ .

II. EXPERIMENTAL DETAILS

The data used in this analysis were obtained from a bubble-chamber experiment carried out at Rutherford High Energy Laboratory by a collaboration of the British Universities of Birmingham, Edinburgh, Glasgow, and Imperial College, London. The Saclay 80-cm bubble chamber filled with liquid deuterium was exposed to a K^- beam. Two exposures were made at 1.45- and 1.65-GeV/ c K^- beam momenta. For the analysis, the data from the two exposures were combined. The details of scanning, measuring, and kinematical fitting, etc. have been given before in Refs. 4 and 5.

In the present analysis following reactions were studied:

$$K^-n(p) \rightarrow \Sigma^0 \pi^-(p), \quad (1)$$

$$K^-n(p) \rightarrow \Sigma^- \pi^0(p), \quad (2)$$

where (p) denotes the spectator proton.

A total of 735 events of type (1), followed by the decay $\Sigma^0 \rightarrow \Lambda \gamma$, and 1478 events of type (2), followed by $\Sigma^- \rightarrow n \pi^-$, were obtained. On the basis of

charge independence, the cross sections and angular distributions for $K^-n \rightarrow \Sigma^0 \pi^-$ and $K^-n \rightarrow \Sigma^- \pi^0$ are expected to be same, which we found to be so in our experimental data; hence, the data of these two reactions are combined together in our analysis.

The selection of K^-n interactions and weighting of Σ events, correction for the decays outside the chamber and very close to the production vertex, and the values of cross section versus energy have been discussed before.⁶

III. PARTIAL-WAVE ANALYSIS

We give here the basic formulas used for the partial-wave analysis. The differential cross section is expanded in a series of Legendre polynomials as

$$\frac{d\sigma(\theta)}{d\Omega} = \lambda^2 \sum_n A_n P_n(\theta),$$

where θ is the angle between the incoming and outgoing meson in the K^-n center-of-mass system, λ is the reduced center-of-mass wavelength, P_n are the Legendre polynomials, and A_n are the Legendre-expansion coefficients.

The coefficients A_n are functions of complex transition amplitude (T 's), i.e., $A_n = \sum_{i \leq j} a_{ij}^n \text{Re}(T_i^* T_j)$, and form a common meeting ground between theory and experiment. To determine these coefficients experimentally, the events selected for the reaction $K^-n \rightarrow \Sigma \pi$ were grouped into bins according to the center-of-mass energy. Bins were chosen to contain sufficient number of events so that reasonable determination of coefficients can be made. The energy of the bin was taken to be the mean energy of the events in that bin. The bin size was different for two samples of events with seen spectators and for all events. The method of moments was employed to calculate the quantities A_n/A_0 and their corresponding errors, for a particular bin. Thus

$$A_n/A_0 = (2n+1) \Sigma \omega P_n(\theta) / \Sigma \omega,$$

TABLE I. Calculated values of coefficients A_n/A_0 ($n = 1, \dots, 8$) in different energy intervals for events with seen spectators and for all events.

Bin limits (MeV)	Mean energy (MeV)	No. of events		A_1/A_0	A_2/A_0	A_3/A_0	A_4/A_0	A_5/A_0	A_6/A_0	A_7/A_0	A_8/A_0	
		Wtd.	Unwtd.									
Seen spectators												
1850-1900	1880	58	55	0.25 ± 0.25	0.82 ± 0.31	-0.37 ± 0.38	0.36 ± 0.43	-0.20 ± 0.49	0.20 ± 0.51	0.01 ± 0.55	0.15 ± 0.55	
1900-1950	1928	130	115	0.78 ± 0.13	0.52 ± 0.17	-0.08 ± 0.21	-0.01 ± 0.26	-0.05 ± 0.28	-0.10 ± 0.30	0.04 ± 0.34	0.81 ± 0.35	
1950-1990	1971	155	147	0.38 ± 0.14	0.36 ± 0.18	-0.17 ± 0.21	0.37 ± 0.24	0.23 ± 0.27	-0.08 ± 0.29	-0.32 ± 0.31	-0.05 ± 0.34	
1990-2015	2002	124	113	0.18 ± 0.52	0.23 ± 0.21	0.03 ± 0.24	0.91 ± 0.27	0.33 ± 0.30	-0.09 ± 0.31	0.15 ± 0.33	0.45 ± 0.33	
2015-2040	2027	159	151	-0.007 ± 0.14	0.55 ± 0.19	0.66 ± 0.23	0.74 ± 0.26	0.47 ± 0.27	0.24 ± 0.30	0.22 ± 0.30	0.20 ± 0.34	
2040-2060	2050	116	109	0.57 ± 0.17	0.87 ± 0.24	0.91 ± 0.30	1.5 ± 0.30	1.23 ± 0.35	0.83 ± 0.44	1.23 ± 0.38	-0.53 ± 0.49	
2060-2100	2078	99	91	0.31 ± 0.18	0.62 ± 0.25	0.71 ± 0.29	1.05 ± 0.30	0.55 ± 0.34	0.33 ± 0.41	0.33 ± 0.40	-0.61 ± 0.43	
2100-2160	2125	98	89	0.81 ± 0.18	1.49 ± 0.24	1.29 ± 0.30	1.52 ± 0.32	0.33 ± 0.38	0.13 ± 0.43	0.45 ± 0.41	-0.41 ± 0.46	
All events												
1850-1920	1893	100	93	0.57 ± 0.17	0.77 ± 0.22	-0.47 ± 0.26	0.10 ± 0.31	-0.73 ± 0.35	-0.12 ± 0.38	-0.18 ± 0.42	0.14 ± 0.43	
1920-1960	1943	136	122	0.74 ± 0.13	0.68 ± 0.18	0.40 ± 0.23	0.46 ± 0.27	0.82 ± 0.28	0.38 ± 0.30	0.58 ± 0.32	0.86 ± 0.34	
1960-1975	1968	97	89	1.06 ± 0.16	0.96 ± 0.25	0.12 ± 0.32	1.04 ± 0.35	0.36 ± 0.40	0.73 ± 0.45	-0.08 ± 0.48	0.46 ± 0.52	
1975-1990	1983	183	168	0.92 ± 0.11	0.49 ± 0.19	0.51 ± 0.32	1.46 ± 0.25	1.60 ± 0.27	0.89 ± 0.31	0.78 ± 0.32	0.94 ± 0.33	
1990-2000	1995	354	328	-0.14 ± 0.09	0.36 ± 0.13	0.59 ± 0.15	0.84 ± 0.17	0.69 ± 0.18	0.46 ± 0.20	0.08 ± 0.22	0.51 ± 0.23	
2000-2015	2006	211	194	0.41 ± 0.11	0.44 ± 0.17	0.38 ± 0.20	1.26 ± 0.22	0.09 ± 0.25	0.54 ± 0.26	0.31 ± 0.28	0.87 ± 0.29	
2015-2035	2024	178	160	0.44 ± 0.13	1.06 ± 0.17	1.26 ± 0.21	1.35 ± 0.25	1.24 ± 0.28	1.08 ± 0.30	1.10 ± 0.31	0.92 ± 0.34	
2035-2060	2048	171	159	0.63 ± 0.14	0.97 ± 0.20	1.22 ± 0.24	1.60 ± 0.24	1.12 ± 0.27	0.95 ± 0.30	0.60 ± 0.33	-0.56 ± 0.38	
2060-2085	2076	257	234	0.68 ± 0.11	0.99 ± 0.16	1.52 ± 0.18	1.58 ± 0.21	1.43 ± 0.23	0.97 ± 0.26	0.84 ± 0.28	0.28 ± 0.30	
2085-2110	2095	170	157	0.88 ± 0.13	1.19 ± 0.19	1.32 ± 0.24	1.52 ± 0.27	0.89 ± 0.31	1.27 ± 0.32	0.79 ± 0.36	0.41 ± 0.38	
2110-2160	2130	85	77	0.96 ± 0.19	1.41 ± 0.26	1.34 ± 0.31	1.36 ± 0.32	0.46 ± 0.37	0.30 ± 0.40	-0.42 ± 0.40	-1.29 ± 0.43	

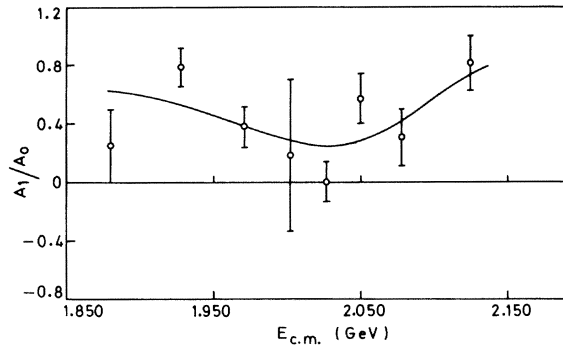


FIG. 1. Experimental value of A_1/A_0 for seen spectators only. The solid curve is the prediction of fit F.

where the sum extends over all events in a given bin, ω being the weight of an individual event, described earlier. As only up to G waves are expected to take part in the interaction in the energy range of this experiment, the maximum value of n was fixed at 8.

The calculated values of coefficients A_n/A_0 in the different energy intervals for events with seen spectators and for all events are given in Table I, along with the bins chosen and weighted and unweighted number of events in the bins.

Figures 1–8 show the data plotted as functions of energy. The curves show the fitted value of fit F, described in Sec. IV.

A. Parametrization of the partial-wave scattering amplitudes and fitting procedure

The amplitude in a given partial wave can be either “resonant” or “nonresonant” (also called

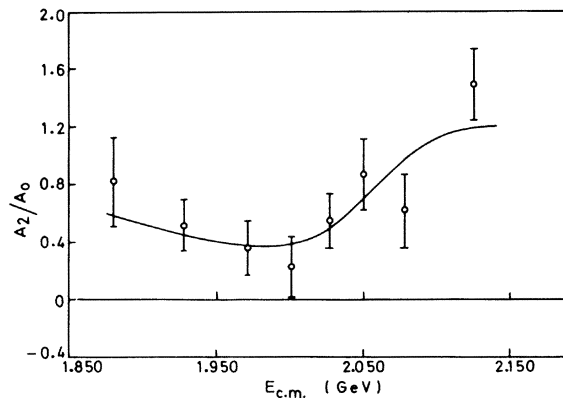


FIG. 2. Experimental values of A_2/A_0 for seen spectators. The solid curve is the prediction of fit F.

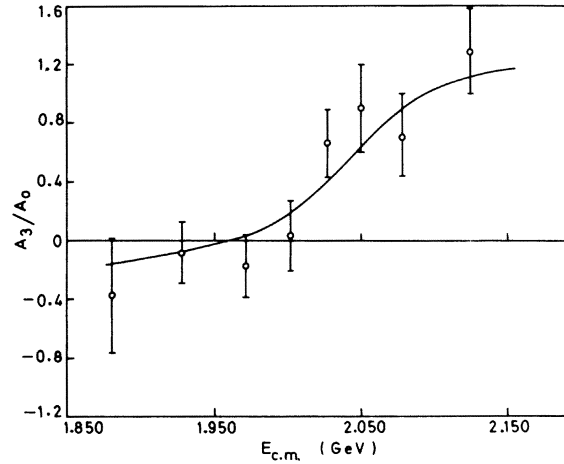


FIG. 3. Experimental values of A_3/A_0 for seen spectators. The solid curve is the prediction of fit F.

“background”) or some combination of both, and their energy dependence was considered in the following manner. The resonant part of the amplitude was given by the Breit-Wigner formula

$$T_R = \frac{\frac{1}{2}e^{i\phi}(\Gamma_e\Gamma_r)^{1/2}}{(E_R - E - i\frac{1}{2}\Gamma)},$$

where Γ , Γ_e , and Γ_r are the total width, elastic-channel partial width, and reaction-channel (here $\Sigma\pi$) partial width, respectively. E_R and E are the resonance and interaction energies, respectively, ϕ is the phase of the resonant amplitude at resonance which was assumed to be either 0 or π , but in certain cases where choice was uncertain the phase was taken as a variable parameter. In this

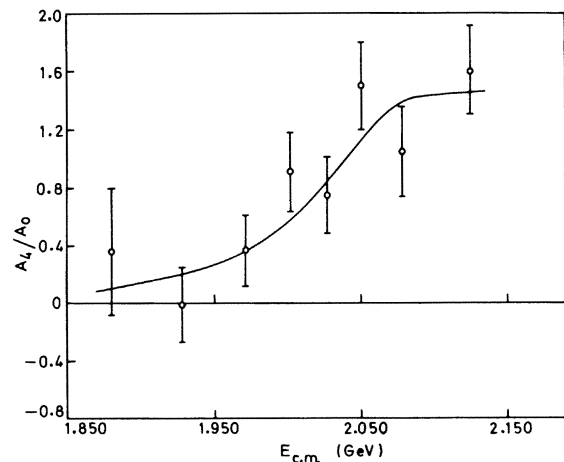


FIG. 4. Experimental values of A_4/A_0 for seen spectators. The solid curve is the prediction of fit F.

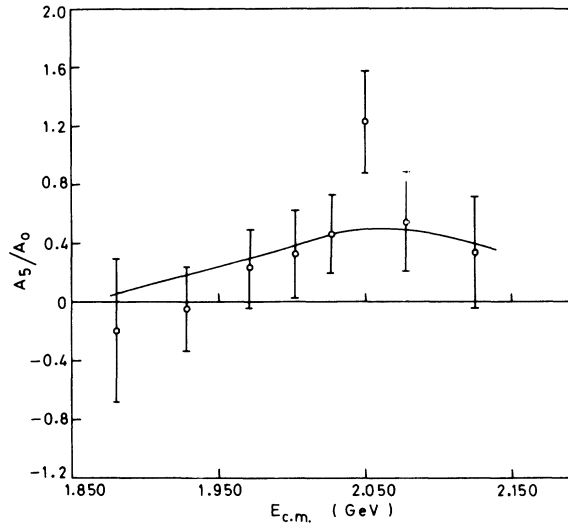


FIG. 5. Experimental values of A_5/A_0 for seen spectators. The solid curve is the prediction of fit F.

analysis all phases have been taken relative to that of $\Sigma(1765)$, the phase of which has been set equal to zero. The energy dependence of the partial width has been approximated as

$$\Gamma_i(E) \propto \left(\frac{k_i^2}{k_i^2 + X^2} \right)^{l_i} \frac{k_i}{E}$$

by Glashow and Rosenfeld,⁷ where X is a mass related to the radius of interaction and is equal to 350 MeV and k_i and l_i are the momentum and orbital angular momentum of the decay product of the resonance in the i th channel. Deans and Holladay⁸ in a fit to total-cross-section data found that 175

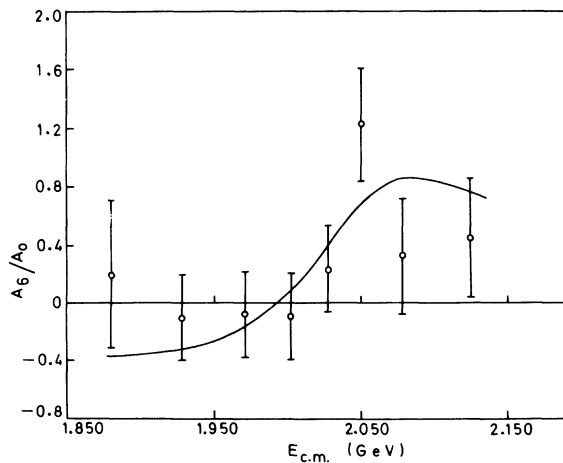


FIG. 6. Experimental values of A_6/A_0 for seen spectators. The solid curve is the prediction of fit F.

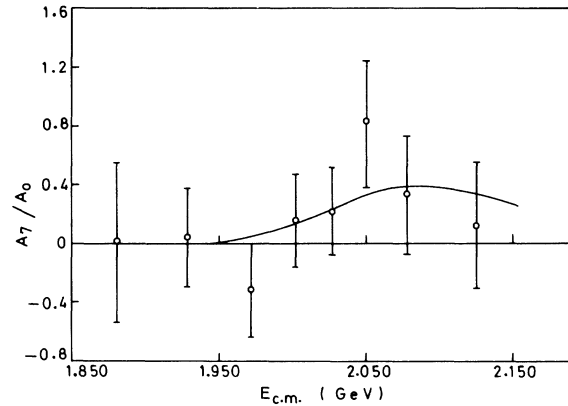


FIG. 7. Experimental values of A_7/A_0 for seen spectators. The solid curve is the prediction of fit F.

MeV was a better value for X . In the present work we take this value of X .^{4,9} We have found in our data that this energy dependence was unimportant because the fits with and without the energy dependence give almost the same values of the parameters.

The nonresonant part of each of the partial-wave amplitudes was parametrized as

$$T_B = (A + Bk) + i(C + Dk),$$

where k is the incident c.m. momentum. For the resonant part of the amplitude the quantities $(x_e x_r)^{1/2} [= (\Gamma_e \Gamma_r)^{1/2} / \Gamma]$, E_R , Γ , and ϕ were variables. If a particular partial wave contained both resonant and nonresonant parts, they were added using the relation

$$T = T_R + T_B.$$

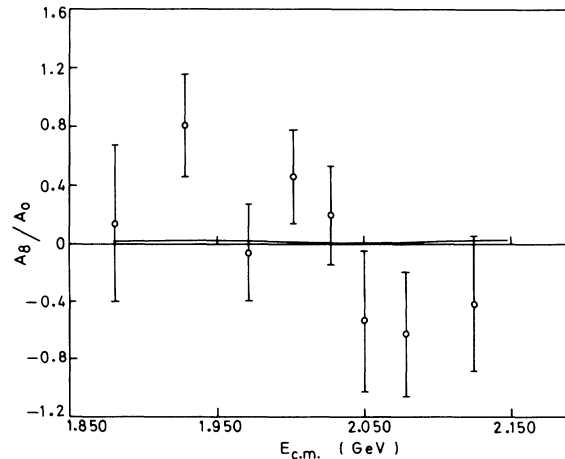


FIG. 8. Experimental values of A_8/A_0 for seen spectators. The solid curve is the prediction of fit F.

The partial-wave analysis was done on an IBM 360 computer. For each fit a hypothesis was made as to which partial waves were resonant. A set of parameters was chosen to describe each hypothesis and reasonable starting values were given for each parameter. These starting values were used to calculate the cross section and angular distributions. The calculated quantity x_c was compared with the observed data point x_0 and their error, Δx_0 , to find χ^2 :

$$\chi^2 = \sum \left(\frac{x_c - x_0}{\Delta x_0} \right)^2.$$

The sum is over all the data points. The χ^2 function was then minimized with respect to all the parameters using CERN minimizing program MINUIT. It may be mentioned that we have neglected the statistical correlations between Legendre coefficients both in the extraction of these coefficients from their events and also in the above-

mentioned definition of the χ^2 function.

After a satisfactory fit was obtained, errors in the fitted values of resonance amplitudes were calculated. This is done by finding the covariance matrix by inverting the second derivative of the χ^2 function; the diagonal elements of the covariance matrix are the squares of the errors.

In doing this, the program assumes that the function is parabolic in all parameters around the minimum. This, however, is not a good approximation. It was found that, in most of the fits, the program found a new minimum with a slight improvement in χ^2 by about 0.5 or less in certain cases. It will then go back to the minimization step and will therefore enter the minimizing routine again and will loop in this way for hours. Each time it will produce a new minimum slightly better than the previous value by about 0.5 or so. Moreover, there was not much change in the resonance parameters. The fitted values reported here are

TABLE II. Summary of fits. Here R denotes a resonance with variable parameters and (R) denotes a resonance with fixed parameters. 1,1 means background of the type $A + iB$ and 2,2 means background of the type $(A + Bk) + i(C + Dk)$, k being incident c.m. momentum.

Fit	S_1	P_1	P_3	D_3	D_5	F_5	F_7	G_7	G_9	χ^2	ν	Prob.
Seen spectators												
A	1,1	1,1	1,1	1,1	1,1	1,1	1,1	1,1	1,1	155	54	0.15×10^{-8}
B	1,1	1,1	1,1	1,1	1,1 (R)	1,1	1,1	1,1	1,1	143.7	54	0.14×10^{-7}
C	1,1	1,1	1,1	1,1	1,1 (R)	1,1	R	1,1	1,1	71.06	53	5%
D	1,1	1,1	1,1	1,1	1,1 (R)	1,1 R	R	1,1	1,1	61.8	50	12.2%
E	1,1	1,1	1,1	1,1 R	1,1 (R)	1,1	R	1,1	1,1	68.2	50	4.4%
F	2,2	2,2	1,1	1,1	1,1 (R)	1,1	R	1,1	1,1	63.9	49	7.4%
G	2,2	2,2	1,1	1,1	1,1 (R)	1,1 R	R	1,1	1,1	87.0	46	0.4%
H	2,2	2,2	1,1	1,1 R	1,1 (R)	1,1	R	1,1	1,1	66.7	46	2.5%
All events												
I	1,1	1,1	1,1	1,1	1,1 (R)	1,1	R	1,1	1,1	228.7	80	
J	1,1	1,1	1,1	1,1	1,1 (R)	1,1 R	R	1,1	1,1	180.9	77	
K	2,2	2,2	1,1	1,1	1,1 (R)	1,1	R	1,1	1,1	180.9	76	
L	2,2	2,2	1,1	1,1 R	1,1 (R)	1,1	R	1,1	1,1	165.7	73	

those reached by the program when successive further entries to minimization improve the χ^2 by less than 0.1. The error estimates were calculated by fixing the parameters of the background at values obtained as above, while the resonant parameters were still allowed to vary. The program then quickly reached a final minimum and found the errors for the resonant parameters.

IV. RESULTS OF PARTIAL-WAVE ANALYSIS

In this section we give the results of the partial-wave analysis. Data were analyzed separately for all events (seen and unseen) and for events with seen spectator protons. The results of the two sets of data are presented separately in Table II. As a first attempt, we assumed that all the amplitudes are nonresonant. The nonresonant amplitudes of the form $T_B = A + iB$, where A and B are complex constants to be determined by the minimizing routine, were assumed in all the partial waves S_1 to G_9 . This gave a χ^2 of 155 for 54 degrees of freedom (fit A) corresponding to a probability of $\approx 10^{-8}$ and is, therefore, very poor representation of the data. In all the subsequent fits, a resonant amplitude was always added in the D_5 wave corresponding to $\Sigma(1765)$ and its parameters were held fixed at values given in Ref. 1, as the data of the present experiment cannot be expected to determine them well. One fit with constant background in all the waves, beside the fixed D_5 resonance, gave a χ^2 value of 143.7 for 54 degrees of freedom (fit B). This was a very poor description of data but was used as a starting point to investigate the effect of adding various resonances to other waves. As the F_7 resonant amplitude, corresponding to well-known $\Sigma(2030)$, is expected to manifest itself in the energy range of the present experiment, the next choice, therefore, was to insert a pure resonant amplitude in the F_7 wave, apart from a fixed resonance in the D_5 wave. In all other waves a constant background was assumed. The parameters E_R , Γ , and $(x_\theta x_\tau)^{1/2}$ of this latter resonance were kept variables. However, the phase ϕ was fixed at π . This resulted in a χ^2 of 71.06 (fit C) for 53 degrees of freedom corresponding to a probability of $\approx 5\%$. Defining the phase, $\phi = 0$, for $\Sigma(1765)$ in this fit and in the remaining fits, the overall phase degeneracy was removed. In all the remaining fits, the F_7 wave was always assumed to be resonant.

Since the $l=1$ total cross section shows a shoulder that is consistent with a resonance of mass 1910 MeV and width 50 MeV,^{10, 11} a resonance of this mass with $J^P = \frac{3}{2}^+$ (Ref. 9) was also added in fit D. With the phase fixed at zero and keeping the resonance parameters E_R , Γ , and $(x_\theta x_\tau)^{1/2}$ variables, minimization yielded a fitted mass of ≈ 1820

MeV and a $\chi^2 = 61.8$ for 50 degrees of freedom, for this fit. This corresponds to a confidence level of 12.2%, but the value of $(x_\theta x_\tau)^{1/2}$ found for this fit is 0.58. It seems unlikely that if such a strong effect really exists, it would not have been observed before. When a F_5 phase $\phi = \pi$ was forced through the parameters, the results so obtained were not so meaningful. In one fit the F_5 phase was varied. It was found that after minimization it approaches very near to zero. When the F_5 parameters were fixed at the best-known values from Ref. 1, this resulted in a totally unacceptable fit as the resonance parameters in F_7 wave diverged to unphysical values. Then a resonant amplitude was also imposed in the P_3 wave, corresponding to $\Sigma(2080)$ along with a pure resonant amplitude in the F_7 wave. The phase of the resonance in the P_3 wave was kept fixed at 0. This gave unacceptable values of the parameters as the value of mass and width of the resonance in the F_7 wave always approached the upper limit set during the process of minimization. The values of the P_3 phase $\phi = \pi$ and variables from 0 to π were also tried but no improvement was found. This, therefore, suggests that the $\Sigma\pi$ decay mode of a P_3 resonance $\Sigma(2080)$ is not favorable, so we omit it from further discussion.

Next we try to detect the formation of the $\Sigma(1940)$ resonance in the D_3 amplitude³ by adding to the linear background in this amplitude, a resonance with free parameters corresponding to $\Sigma(1940)$. All other waves are parametrized as in fit C. This gives a total of 22 variables and 50 degrees of freedom. This improved the χ^2 to a value of 68.2 for 50 degrees of freedom corresponding to a probability of 4.4% (fit E) which is reasonably good. The fitted parameters of $\Sigma(2030)$ remain essentially the same as in fit C. When a fit was attempted with a resonance added to both S_1 and D_3 waves, the parameters diverged to totally unacceptable values and a very bad fit was obtained.

In the second group of fits linear background is tried in some partial waves. Other partial-wave analyses (e.g., Refs. 4 and 9) have shown that S_1 and P_1 amplitudes in particular have considerable energy dependence. The fit F is similar to fit C but the constant background used in fit C is replaced by the amplitudes with real and imaginary parts linear in c.m. momenta in the S_1 and P_1 waves. The probability for this fit is considerably increased, reducing the χ^2 to 63.9 for 49 degrees of freedom. Then with the addition of a resonance in the D_3 wave (fit H) the probability is slightly decreased. When a fit was attempted with energy-dependent background in the S_1 and P_1 waves and a resonant amplitude in the P_3 and F_7 waves, unacceptable values were found for the F_7 resonance. Each time its mass and width approach the upper

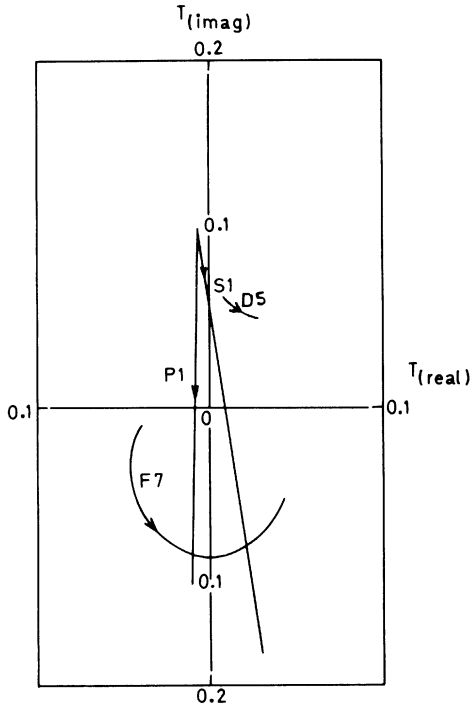


FIG. 9. Argand diagram of the fitted partial-wave amplitudes in fit F.

limit. Figure 9 displays the Argand-diagram plot of fitted amplitudes in fit F.

Since eight amplitudes are involved in this study and in order not to increase prohibitively the number of parameters to be determined, the linear parametrization of the background was a reasonable compromise with the statistics of this experiment.

Some of the fits mentioned above were also carried out with the coefficient ratio A_n/A_0 obtained using all events. With the inclusion of unseen-spectator events, the statistics was almost dou-

bled. Here the total number of events were divided into 11 energy bins rather than the 8 used for the events with seen spectator only. Therefore, the total number of data is 27 more. In all the fits using data with all events (fits I to L), the probability is quite low, for example, when fit C was attempted with all events (fit I) a χ^2 of 228.7 for 80 degrees of freedom was obtained, resulting in a very low probability. But the values of the resonance parameters are not substantially changed. Similarly, fit D was also tried with all events (fit J) and a χ^2 of 180.7 for 77 degrees of freedom was obtained. Fit K, which has a resonance in the F_7 wave, gave a χ^2 of 180.9 for 76 degrees of freedom. But the fitted values of mass and width for the F_7 resonance were low compared to the similar fit with seen spectator events. In fit L, a χ^2 of 164.7 for 73 degrees of freedom was obtained. The values of the resonance parameters were similar to those obtained in a similar fit with seen-spectator events (fit H).

As the events with unseen spectators have larger errors and are more contaminated, therefore, we have introduced the resonances in some important waves only. The resonance parameters for D_3 and F_7 waves obtained in two sets of data are similar.

V. CONCLUSION

We have listed in Table II various fits and the probabilities of their occurrences. Of all the fits listed in the Table II, the one with highest probability ($\approx 12\%$) has a variable resonance in the F_5 and F_7 waves (fit D) and constant background in all the waves except F_7 . The resonant structure seen in the F_5 wave has fitted values of mass ~ 1820 MeV which lies at the lower boundary of our energy range and therefore cannot be supported by our data. Because of this, fit F with a variable resonance in F_7 and probability of $\approx 7\%$ is preferable to fit D even though the latter is statistically better. In all the fits, except D, the mass of the resonance

TABLE III. Selected fits for the resonance parameters.

Fit	F_7 ($\phi = \pi$)		$e^{i\phi}(x_e x_r)^{1/2}$ ^a	D_3 ($\phi = 0$)		
	E_R (MeV)	Γ (MeV)		E_R (MeV)	Γ (MeV)	$e^{i\phi}(x_e x_r)^{1/2}$
C	2057.8 ± 7	195_{-22}^{+26}	-0.099 ± 0.006			
D ^b	2027.0 ± 5	126.3_{-19}^{+24}	-0.07 ± 0.006			
E	2053.2_{-7}^{+9}	187.0_{-23}^{+29}	-0.099 ± 0.006	1997.1_{-3}^{+5}	72.3 ± 14	$0.03_{-0.015}^{+0.02}$
F	2056 ± 8	176.6_{-26}^{+32}	-0.085 ± 0.006			
H	2057 ± 9	176.7_{-28}^{+33}	-0.09 ± 0.007	1979.6_{-12}^{+11}	72.47_{-23}^{+40}	0.037 ± 0.001

^aThe error quoted is only statistical as given by the minimizing routine.

^bIn fit D, a resonance was also imposed in the F_5 wave.

in F_7 is in the region of 2050 MeV, slightly higher than the world average of 2030 MeV and the width is ≈ 180 MeV. In fit D, where a resonance is imposed in the F_5 wave, the mass and width of resonance in F_7 is lowered down to 2027 and 126 MeV, respectively.

The quantities describing the resonance parameters, i.e., E_R , Γ , and $e^{i\phi}(x_e x_r)^{1/2}$ for some selected fits are given in Table III. On the basis of these fits we can draw the following conclusions:

The mass and width of $\Sigma(2030)$ lie in the range

$$E_R \approx 2027 \text{ to } 2057 \text{ MeV,}$$

$$\Gamma \approx 126 \text{ to } 195 \text{ MeV,}$$

and the branching fraction in the $\Sigma\pi$ decay mode is $e^{i\phi}(x_e x_r)^{1/2} = -0.085 \pm 0.015$, which also happens to be the central value on the basis of best fit F in our own data. The error indicates the spread of the values for different fits which arises due to the

variation in the type of the background and its parametrization. Taking into account an additional systematic error of about 0.01 due to the neglect of Legendre coefficient correlations, we would like to quote a value of $e^{i\phi}(x_e x_r)^{1/2} = -0.085 \pm 0.02$.

Further, on the basis of fits E and H the resonance in the D_3 wave is confirmed with mass ≈ 1990 MeV and width ≈ 72 MeV in agreement with Kane.³

ACKNOWLEDGMENT

We are grateful to the members of British Collaborating Universities for allowing us the use of data analyzed in the present work. In particular, D. P. Goyal would like to express his gratitude to Professor Ian Butterworth, Professor S. J. Goldsack, and Dr. D. B. Miller for their kind hospitality at Imperial College. Financial assistance from Department of Atomic Energy, Government of India, is gratefully acknowledged.

¹Particle Data Group, Rev. Mod. Phys. 48, S1 (1976).

²A. Berthon *et al.*, Nucl. Phys. B24, 417 (1970).

³D. F. Kane, Phys. Rev. D 5, 1583 (1972).

⁴G. F. Cox *et al.*, Nucl. Phys. B19, 61 (1970).

⁵D. C. Colley *et al.*, Nucl. Phys. B31, 61 (1971).

⁶D. P. Goyal and A. V. Sodhi (unpublished).

⁷S. L. Glashow and A. H. Rosenfeld, Phys. Rev. Lett.

10, 192 (1963).

⁸S. R. Deans and W. G. Holladay, Bull. Am. Phys. Soc.

11, 516 (1966).

⁹W. M. Smart, Phys. Rev. 169, 1330 (1968).

¹⁰R. L. Cool *et al.*, Phys. Rev. Lett. 16, 1228 (1966).

¹¹J. D. Davies *et al.*, Phys. Rev. Lett. 18, 62 (1967).